J Musculoskel Neuron Interact 2003; 3(2):176-184

Original Article

Hylonome

A micro-computed tomography study of the trabecular bone structure in the femoral head

A.S. Issever[1], A. Burghardt[1], V. Patel[1], A. Laib[1], Y. Lu[1], M. Ries[2], S. Majumdar[1]

[1]Magnetic Resonance Science Center, Department of Radiology, University of California, San Francisco, USA,
[2]Department of Orthopaedic Surgery, University of California, San Francisco, USA

Abstract

The goal of this study was to characterize the trabecular microarchitecture of the femoral head using micro-computed tomography (μCT). Femoral head specimens were obtained from subjects following total hip replacement. Cylindrical cores from the specimens were scanned to obtain 3-D images with an isotropic resolution of 26 μm. Bone structural parameters were evaluated on a per millimeter basis: relative bone volume (BV/TV), trabecular number (Tb.N), thickness (Tb.Th) and separation (Tb.Sp), structure model index (SMI), and connectivity (Conn.D). The μCT data show that the first two millimeters, starting at the joint surface, are characterized by more plate-like trabeculae, and are significantly denser than the underlying trabecular bone. Regional differences in the trabecular architecture reveal that the superior pole has significantly higher BV/TV, Tb.N and Tb.Th values, with lower Tb.Sp compared to the inferior and side poles. Because subchondral bone is essential in the load attenuation of joints, the difference in bone structure between the subchondral and trabecular bone might arise from the different functions each have within joint-forming bones. The denser trabecular structure of the superior pole as compared to the inferior pole can be interpreted as a functional adaptation to higher loading in this area.

Keywords: Femur, Bone, Micro-Computed Tomography (microCT), Osteoarthritis, Trabecular Structure

Introduction

The hip, particularly the femur, is a predisposed site for symptoms of orthopaedic disease. In our present study we have focused on analyzing the trabecular bone structure of femoral heads with osteoarthritis (OA).

OA is a major cause for joint dysfunction in the elderly, and is associated with severe pain and immobility[1,2]. In its late stages OA is the most frequent indication for total hip arthroplasty[3]. Dominating anatomical changes in OA include osteophytes and cartilage deterioration with eventual exposure of sclerotic subchondral bone. As a result of pathological overloading and malnutrition, compressional micro-fractures in this bone region are frequent, leading to the formation of pseudocysts[4]. As younger patients also suffer from OA, the "wear and tear" explanation is not sufficient. Simplistically, OA is the result of the joints' inability to withstand mechanical loading. The joint is an anatomical structure composed of many elements such as bone, cartilage, ligaments, muscles, synovial tissues, and liquid. It is therefore likely that OA is a multifactorial disease. The major question that remains to be answered is how the different joint-forming tissues act in the initiation and progression of OA.

An idea that has evolved in recent years is that cartilage and subchondral bone form a tight functional unit and that OA is a disease of this unit. Whether changes in the cartilage or in the subchondral bone initiate the process is unknown. Radin et al. have shown that subchondral bone as compared to articular cartilage is of essential importance for the attenuation of loading in the joint[5], proposing that early cartilage degeneration, as seen in OA, is associated with changes in the subchondral bone's ability to absorb impact[6]. McKinley and Bay showed that trabecular strain distribution is altered by induced cartilage defects and that these changes can be site specific[7]. Dieppe et al. showed, with scintigraphical techniques, an increased subchondral bone metabolism in arthritic knees[8], further supporting the theory that subchondral bone changes are significant in the development of OA.

In a more general view of how OA presents itself, it is

Corresponding author: Sharmila Majumdar, PhD, Department of Radiology, Magnetic Resonance Science Center, University of California, San Francisco, 1 Irving Street, AC-109, San Francisco, CA 94143-1290, USA
E-mail: sharmila.majumdar@mrsc.ucsf.edu

Accepted 29 January 2003

gender	age	Noyes Scale	Cartilage [mm]			BMD [gr/cm^2]	
			superior	inferior	side	superior	inferior
male	90	III A	0.74	1.50	1.35	0.46	0.29
male	56	III A	0.00	1.97	---	0.30	0.23
male	56	III A	0.20	1.11	2.18	0.28	0.23
male	52	III B	1.63	1.44	0.88	0.22	---
female	60	III A	0.25	1.58	2.45	0.26	0.18
male	73	III A	0.00	3.11	1.72	0.28	0.22
female	71	III B	0.80	2.62	2.63	0.20	0.18
female	66	III A	0.69	1.84	2.50	0.20	0.26
male	61	III A	0.00	1.49	2.22	0.28	0.26

Table 1. Age, gender and Noyes Scale of each femoral head and the average cartilage thickness and bone mineral density of the respective superior, inferior and side pole cores.

known for hip OA that the cartilage degeneration of the proximal femur shows regional differences[9,10]. Specific areas of the femoral head consistently show higher cartilage degeneration than others, suggesting a regional dependency of OA. In physiologically healthy conditions, the main structural function of the proximal femur can be summed up as the transfer of body weight from the pelvis onto the lower limb, providing the body with maximum stability in static as well as in dynamic conditions. In addition to the body weight, forces of attached muscles and ligaments form the overall load that acts upon the femoral head.

For the load distribution within the femoral head itself, multiple factors, such as tissue composition, geometry, load direction, and magnitude have to be considered. Different regions of the femoral head undergo different mechanical stresses and loading. We can identify regions in which compressive loading prevails more than in others[11]. The different tissue types will adapt to the mechanical loading with corresponding structural changes according to Wolff's Law[12]. Specifically for the bone component of the femoral head, those adaptive processes will most likely be detectable in the subchondral and trabecular bone structure. Therefore, we hypothesize that regions within the femoral head will differ in their trabecular microarchitecture due to the different mechanical stress and load.

Using micro-computed tomography, a newly developed imaging modality, the aim of this study was twofold: i) to observe three-dimensional changes in microarchitecture as a function of depth from the joint surface, enabling analysis of subchondral bone and trabecular bone architecture, ii) to show regional microarchitectural differences in the subchondral and trabecular bone of the femoral head (i.e. superior versus inferior versus side poles) in the femur of subjects with OA.

Material and methods

Specimens and preparation. Nine femoral heads were obtained from 8 subjects (three female, five male) who underwent total hip replacement (one subject having a bilateral total hip replacement). The average age was 65 years and ranged from 52 to 90 years. For all subjects, indication for the surgery was degenerative osteoarthritis of the hip.

The femoral heads were visually evaluated by an orthopaedic surgeon for their grade of cartilage lesion using the following modified Noyes Scale: IA - focal cartilage softening; IB - extensive cartilage softening; IIA - fissuring with cartilage thinning of about 50%; IIB - fissuring with cartilage thinning of more than 50%; IIIA - full cartilage thickness loss; IIIB – full cartilage and bone loss (Figure 1).

With a water-cooled diamond tipped drill bit we obtained 38 cylindrical cores from the femoral heads, each with a diameter of 7 mm and a height varying from 14 mm to 31 mm. The diameter of the core was selected such that it could be accommodated within the BCT scanner, and could be imaged at the highest possible resolution. The cores included (if existing) articular cartilage, cortical, subchondral and trabecular bone. A total of 15 cores from the superior pole (superior to the fovea capitis femoris), 8 from the inferior pole (inferior to the fovea capitis femoris), and 15 from the side poles (anterior and posterior side of the femoral head) were acquired (Figure 2). The cores were stored in a 10% formalin-saline solution.

Bone mineral density measurements and X-ray imaging. Bone mineral density is often considered a necessity in bone studies, as it is a methodology that can be easily extended to the clinical realm. In order to document these measures of BMD, and their correspondence to our high resolution studies, BMD was measured in a subset (23 cores) from the superior and inferior pole. The measurements were made using a clinical dual energy X-ray absorptiometer (DEXA) (Hologic QDR-4500A, Bedford, Massachusetts, USA) with a standard AP spine scan mode. Analysis was performed using the low density spine software with rectangular regions of interest.

Planar radiographs were taken of all cores with a voltage of 50 kVp and an exposure time of 100s.Using the 7 mm core diameter as a calibration, the cartilage thickness was determined from the digitized radiographs at three locations, as seen in Figure 3.

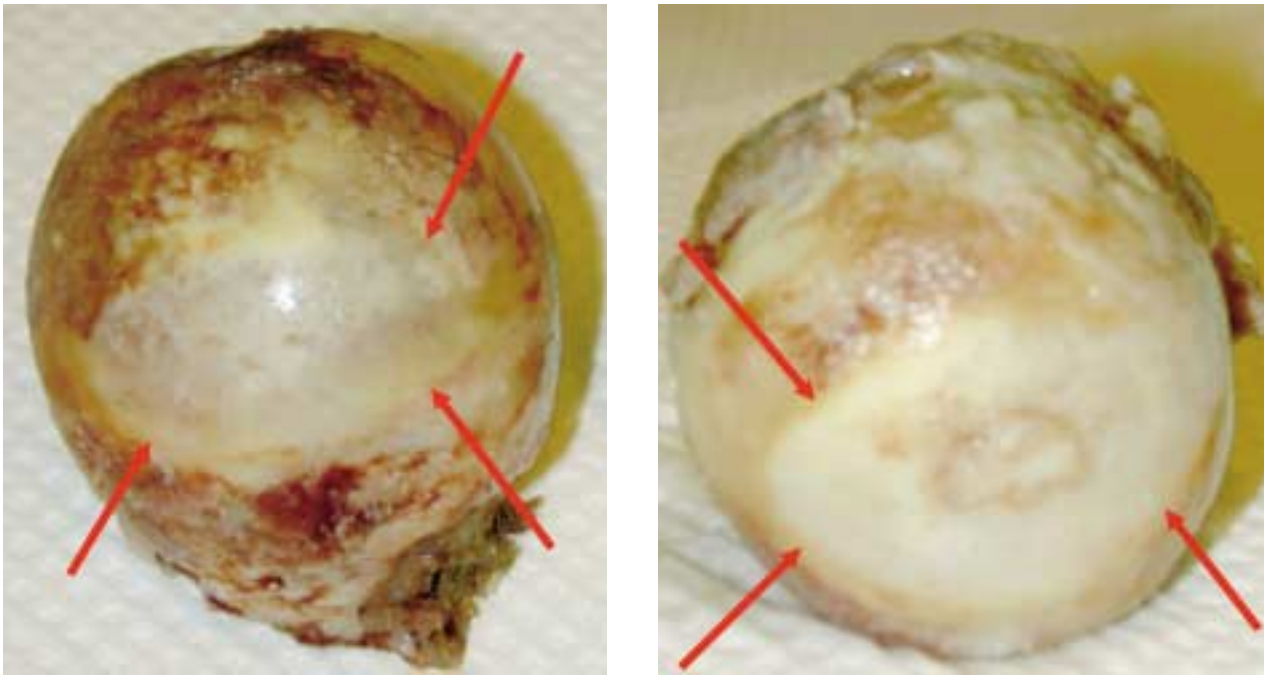

Figure 1. Representative images of Noyes Scale III A (A) and B (B) graded femoral heads. The arrows indicate the border of cartilage degeneration. On Figure B bone is exposed.

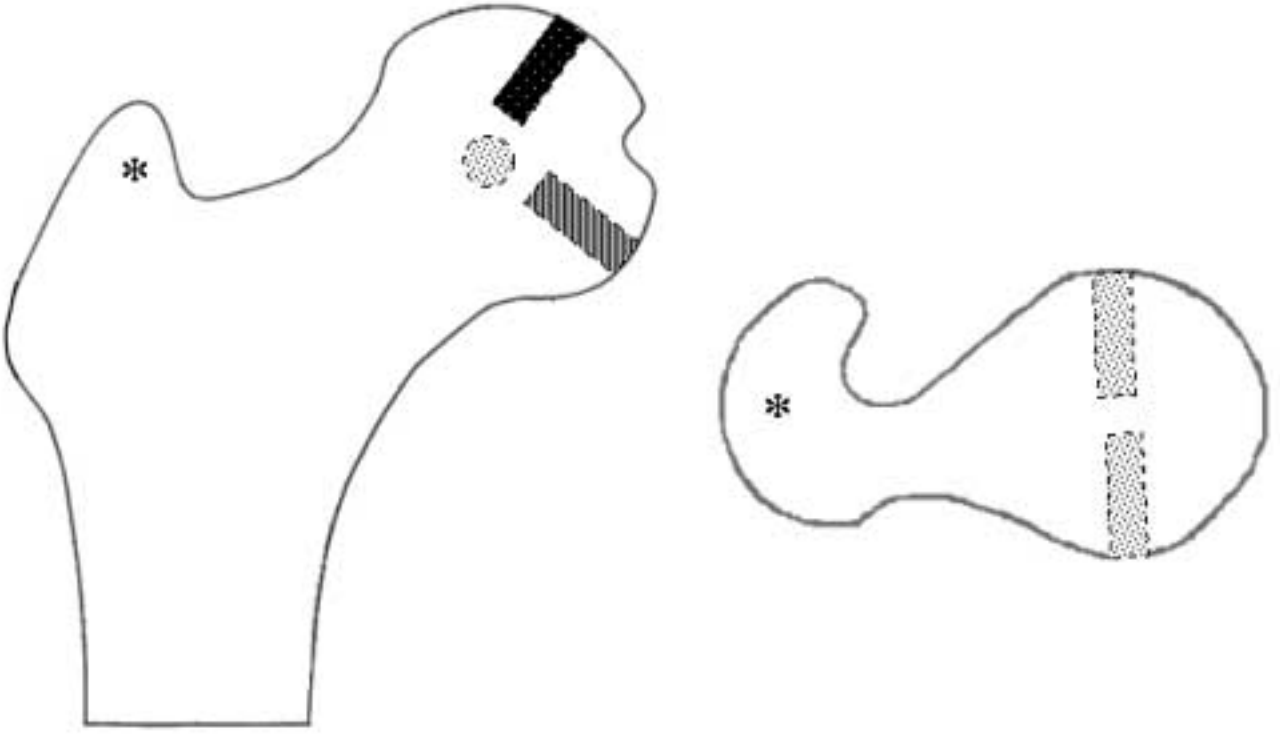

Figure 2. Diagram showing the location of the sample sites. Cores were extracted from the superior pole (black), inferior pole (dark grey), and side poles (light grey).

Figure 3. Representative X-ray image of sample, showing the sites used for cartilage thickness determination.

Micro-computed tomography (μCT) imaging. The cores were scanned in plastic vials, immersed in a 10% formalin-saline solution using a high resolution MicroCT system (μCT-20, Scanco Medical, Bassersdorf, Switzerland). Images were obtained with a cubic voxel size of 26 μm and regions of interest were placed within trabecular bone, starting beneath the bone surface[13]. The resulting gray level images were binarized into a bone and marrow phase by first applying a low pass Gaussian filter (width = 0.5, support = 1 or a kernel size of 3) to remove noise and then using a single, manually selected threshold for all samples. The following three-dimensional structural parameters were calculated for consecutive millimeter increments, starting at the joint surface: relative bone volume (BV/TV), trabecular number (Tb.N), thickness (Tb.Th) and separation (Tb.Sp), structure model index (SMI), and connectivity (Conn.D). The data analysis on a per millimeter basis enabled us to analyze and describe structural dependencies as a function of depth.

Tb.Th, Tb.Sp and Tb.N were assessed using the distance transformation method described by Hildebrand et al.[14], i.e. Tb.Th was calculated as the mean diameter of spheres filling the trabecular structure, while similarly Tb.Sp was calculated as the mean diameter of spheres filling the marrow phase. Inversing the mean diameter of spheres filling the skeletonized structure resulted in the Tb.N. The Structure Model Index (SMI), a parameter describing the general shape of the structure, was calculated as follows[15]:

$$SMI = 6 \cdot \frac{BV \cdot \frac{dBS}{dr}}{BS^2}$$

BV (bone volume) and BS (bone surface area) are calculated from a surface generated by a triangle meshing technique based on the Marching Cubes method[16], and dBS/dr is determined by calculating the differential change in BS as the surface triangles are extended along the direction of the surface normals. The theoretical SMI value for a perfect cylinder (rod) is 3, while a perfect plate is 0. Negative SMI values are possible when the surfaces become increasingly concave (i.e. the dBS/dr factor becomes negative), as is seen in high density subchondral bone, or in regions with fenestrations and remodeling, in a plate-like structure. Furthermore, Conn.D was determined by calculating the Euler number after removing any extraneous unconnected elements[17].

The X-ray source in the BCT scanner was not monochromatic, and no calibration phantom has been validated thus far, hence the extent of mineralization was not determined from the BCT scans.

Statistical analysis. The data were transferred to a Microsoft Windows based system and tabulated using Excel software. Depth based and regional dependent analysis was performed. Statistical analysis included the Renitex model with F-test analysis of variance. Tabulated values included p- and t-test values and the Pearson product correlation moment coefficient.

Results

Cartilage and orthopaedic assessment. All specimens were graded as Noyes III, revealing full cartilage thickness loss, with two including bone loss (Noyes III B). The evaluation of the X-ray images (such as shown in Figure 3) reveals that the highest cartilage deterioration is found at the superior pole. With average cartilage thicknesses of 0.59 mm for the superior pole, 1.74 mm for the inferior, and 1.85 mm for the side poles, the t-test ($p<0.05$) shows that the differences between the superior pole, compared with the inferior and side poles are highly significant, while the inferior pole and the side pole show no significant difference from each other. The DEXA measurements show that samples from the superior pole (BMD=0.28 gr/cm^2) have significantly higher BMD values ($p=0.05$) as compared to the inferior pole (BMD=0.23gr/cm^2). In the superior pole region the correlation between BMD and cartilage thickness is significant ($r=-.50$), whereas for the inferior pole no significant correlation ($r=0.007$) was found. Table 1 summarizes the data of each femoral head.

μCT results. Figure 4 shows representative images of cores from the same femoral head, depicting the differences in trabecular bone structure in different regions, and depths of the femoral head.

Subchondral and trabecular bone structure relative to depth:

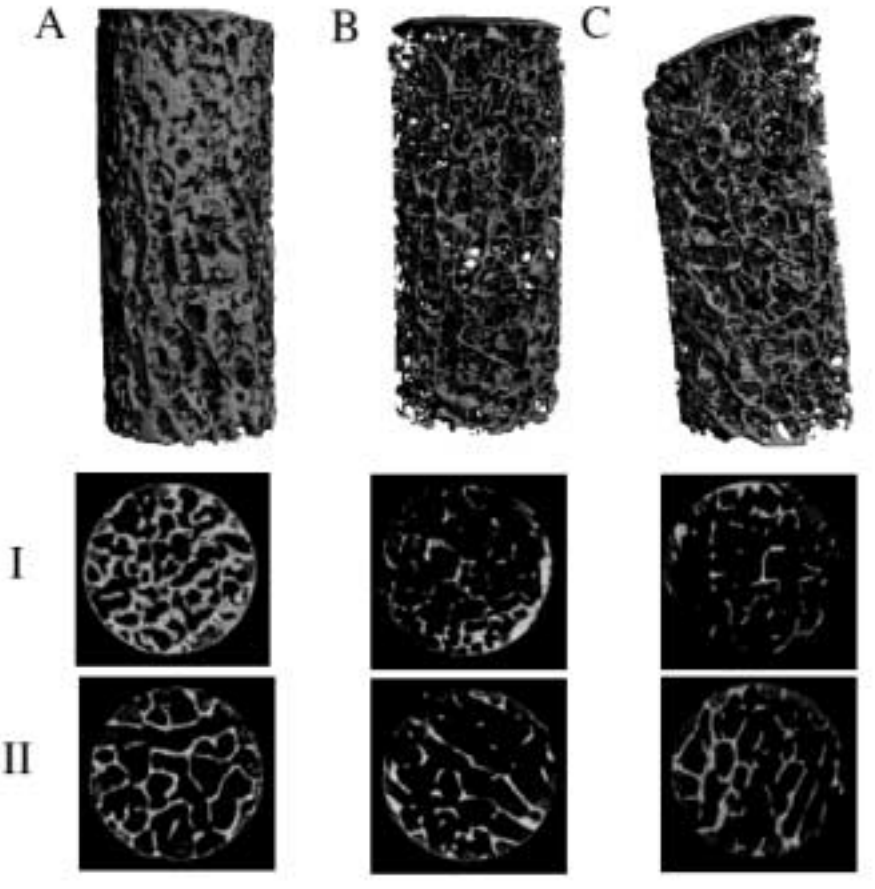

Figure 4. 3-D μCT reconstruction of representative cores (superior pole [A]; inferior pole [B]; side pole [C]) of the same femoral head and cross sectional μCT images at a depth of 1.5 mm [I] and 12 mm [II] from the joint surface.

For each location, Figure 5 A-F shows the mean values of the structural parameters plotted as a function of depth. A range from 0 to 15 mm starting right beneath the cortical shell is covered. It can be seen that the most prominent changes occur within the first millimeter of the samples. For BV/TV, Tb.N, and Tb.Sp this is highly significant ($p<0.0001$) for the first two millimeters. After approximately the first five millimeters, depending on the parameter, a steady decreasing (e.g. BV/TV, Tb.N) or increasing (e.g. Tb.Sp, SMI) trend from the superior to the inferior pole is observed. The superior pole graphs and the inferior/side pole graphs converge with each other at greater depths, as they aim towards the center of the femoral head. For the whole femoral head (superior, inferior, and side pole), the number of trabeculae (Tb.N) is highest close to the joint surface. Consequently Tb.Sp in this depth region is rather low and BV/TV is high. With increasing depth from the joint surface, Tb.N and BV/TV initially decrease rapidly while Tb.Sp increases. For Conn.D and SMI a similar behavior can only be found for the inferior and side pole. Here the trabecular network shows higher connectivity with rather plate-like trabeculae close to the joint surface. With depth, connectivity decreases and the trabeculae become more rod-like. Interestingly, Tb.Th is the structural parameter that shows the least significant depth-dependent variations.

Regional changes/differences (superior versus inferior versus side pole): Differences in structural parameters due to regional factors (superior, inferior, and side pole) are highly significant (for p-values see Table 2). The figures show that the inferior and side pole are closely linked to each other; their structural parameters do not differ in a statistically relevant manner, with one expectation being for Tb.Th in depths greater than five millimeters. Compared to these, the superior pole shows highly significant increased values for BV/TV, Tb.N, and Tb.Th with lower Tb.Sp. In regions near the joint the values for Conn.D of the superior pole do not differ from the inferior and side pole, but with depth it can be seen that the superior pole has higher Conn.D values.

Cartilage/structure relationship: The Pearson correlation coefficients calculated (see Table 3) show strong negative correlations for cartilage thickness with BV/TV, Tb.Th, and Tb.N. Positive correlations were seen with Tb.Sp and SMI. Finally the Pearson correlation coefficient was also calculated to examine the cartilage thickness, BMD relation. This was also found to be negatively correlated with cartilage thickness, though not as strongly as BV/TV.

		sup. vs. inf.	sup. vs. side	inf. vs. side
BV/TV	Region 1	0.0015	0.0053	0.1252
BV/TV	Region 2	<0.001	< 0.001	0.2933
Tb.N	Region 1	0.0218	0.0814	0.3833
Tb.N	Region 2	<0.001	<0.001	0.5534
Tb.Th	Region 1	0.0020	0.0017	0.1673
Tb.Th	Region 2	<0.001	0.001	0.001
Tb.Sp	Region 1	0.0096	0.0439	0.7341
Tb.Sp	Region 2	<0.001	<0.001	0.8699
SMI	Region 1	0.0090	0.0055	0.1969
SMI	Region 2	<0.001	<0.001	0.3927
Conn.D	Region 1	0.9638	0.7666	0.1766
Conn.D	Region 2	<0.001	<0.001	0.0721

Table 2. Paired t-test values (p-values) for superior vs. inferior vs. side pole comparison over the first 3 mm (Region 1) and 4-15 mm (Region 2).

Parameter	Pearson correlation coefficient (r) For Cartilage Thickness
Conn.D	0.0634
BV/TV	-0.5785
Tb.Th	-0.6398
Tb.Sp	0.4315
Tb.N	-0.3671
SMI	0.6160
DEXA-BMD	-0.4628

Table 3. Pearson correlation coefficients (r) calculated for each structural parameter over the first 2 mm against cartilage thickness.

Discussion

Changes seen as a function of depth. The results show that for all regions, the greatest rate of change for the structural parameters occurs within the first two millimeters (subchondral bone). Compared to trabecular bone, subchondral bone is structurally characterized by an increased number of plate-like trabeculae. Subchondral bone is of essential importance for the biomechanical function of the joint. Radin et al.[5,6] have shown that subchondral bone absorbs most of the impact under joint loading and distributes this load onto the underlying trabecular bone structure. Assuming that within the femoral head there are two structural compartments which are different in volume size (the rather thin outer fringe of subchondral bone and the inner trabecular bone), and considering that both of these compartments have to bear the same load, it is obvious that within the subchondral bone, the "load / volume" ratio is much higher than in the trabecular bone. According to Wolff's Law[12], this will lead to adaptive bone turnover processes, with increased density of the subchondral bone structure as seen in our results. The question arises why there is, after the first initial millimeters, such an abrupt change in the bone structure. What is the significance of two structurally different types of bone not only within the femoral head but for all joint-forming bones, if both types bear, respectively transfer the same load? A possible answer suggested by recent stud-

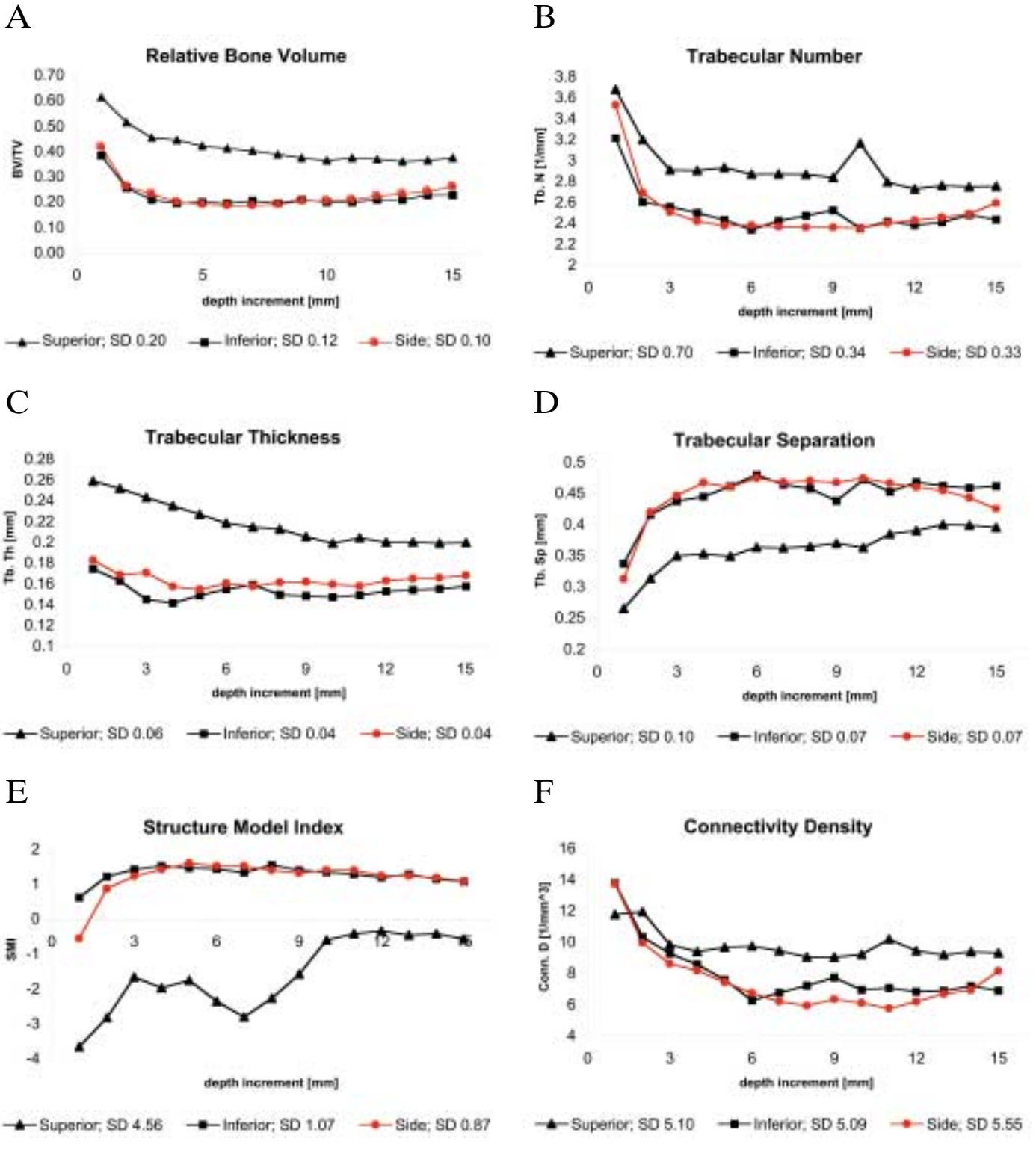

Figure 5. Mean values of structural parameters (y-axis) plotted as a function of depth in millimeter increments from the joint surface (x-axis), with average standard deviations (SD) in legend [BV/TV (A); Tb.N (B); Tb.Th (C); Tb.Sp (D); SMI (E); Conn.D (F)].

ies is that subchondral bone is not only essential for mechanical purposes, such as absorbing and transferring load, but also has other functions within the joint itself, that are not carried out by the trabecular bone. As described by Imhof et al., subchondral bone is highly vascularized and it is closely connected with the basal layers of cartilage via vascular channels, supplying the deeper cartilage zones with additional blood flow[18]. It seems that the cartilage and the under-

lying subchondral bone form a tight functional unit. Although histologically they belong to different tissue types, they influence each other mutually.

Regional differences. Regional differences in the structural parameters of the subchondral and trabecular bone are highly significant. The superior pole compared to the inferior and side poles shows a denser structure. As the inferior and side poles do not differ structurally from each other, focus will for reasons of simplicity, be on changes seen between the superior and inferior poles. Greenwald et al. have described a region of the femoral head which independent of the position predominately articulates, with the acetabulum at large loads. This region is located in the area from which we took our superior pole samples. Likewise the area from which we obtained our inferior pole samples has been described by Greenwald et al. as an area of habitual non-contact, which does not articulate with the acetabulum in any position and any load[19]. We can presume therefore, that the superior pole of the femoral head is the load-bearing pole, where high compressional forces act, whereas the inferior pole is the non-load-bearing region of the femoral head. According to Wolff's Law higher mechanical loading leads to a positive bone turnover which is reflected in the trabecular microarchitecture of the superior pole. As described in the results the superior pole is more dense, with higher values in Tb.N, Conn.D, and Tb.Th. while Tb.Sp is eventually lower. The negative SMI values in the superior pole show that the dense structure in this region has more concave than convex surfaces while the inferior and side poles show plate or rod-like structures with convex surfaces (Figure 6). The increased density of the superior pole is also reflected in the higher BMD values as assessed by our DEXA measurements.

This study does not, however, document the heterogeneity as a function of specimen size in each of these poles of the femur. We were restricted in core diameter by the resolution we wished to achieve for all our studies in the BCT scanner. Doubtless, adjoining regions in the superior pole show a continuous change or variation in bone structure, but this was within the scope of this study.

Cartilage/bone relationship. The correlations between the measured cartilage thickness and the various structural parameters suggest a structural thickening process is linked with cartilage degeneration. BV/TV and Tb.Th in particular are strongly linked to changes in cartilage thickness while Tb.N is less so and the correlation with connectivity is very weak. This suggests the increase in bone density may be the result of structural thickening as opposed to the addition of new trabeculae. The strong positive correlation for SMI also potentially indicates that subchondral sclerosis is linked with cartilage degeneration.

Conclusion

Previous studies have described the relationship between cartilage degeneration and increased stiffness of the underlying subchondral bone. Radin et al. proposed that steep stiffness gradients within subchondral bone propagate through the cartilage and lead to cartilage degeneration through overloading. As we have not performed mechanical tests on our samples, we can not make statements about the stiffness, but clearly our results show that the subchondral bone of the superior pole is much denser than the inferior pole. If we presume that higher trabecular density is linked to increased stiffness we can explain the higher rate of cartilage deterioration in the superior pole samples as seen on our X-ray images.

Recent studies have shown that changes in subchondral bone are closely linked to cartilage changes[20,21]. In this study, it was not possible to harvest "normal" cadaveric specimens, as our tissue bank had age-matched controls which either had hip pathology, such as avascular necrosis, or fracture, and young donors were typically trauma cases. Thus, since we only included osteoarthritic samples, our results focus on regional changes within the femoral head, showing that certain regions are subjected to higher cartilage deterioration

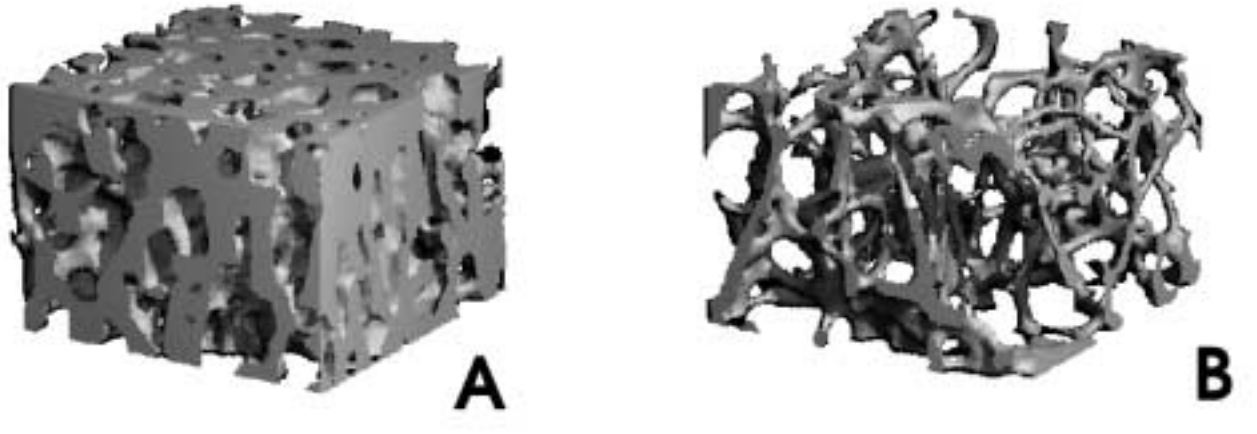

Figure 6. 3-D renderings showing subchondral bone near the articular surface of the superior pole with SMI < 0 (A) and trabecular bone 12 mm from the articular surface of the inferior pole with SMI > 0 (B).

and denser bone structure than others in the degenerative hip joint. To understand the chronology of this process, whether cartilage changes precede the bony changes, or vice versa, in OA, warrants further *in vivo*, longitudinal studies, using methods such as magnetic resonance or perhaps high resolution spiral computed tomography coupled with magnetic resonance.

Acknowledgments

The authors thank John Shepherd (PhD) for his assistance with the bone mineral density measurements and Katherine Hall, Jessica Gibbs and Andrew Philipoff for support. This work was supported and funded by NIH grant RO1 AG 17762.

References

1. Dieppe P. Fortnightly Review: Management of hip osteoarthritis. BMJ 1995; 311:853-857.
2. Peyron J. The epidemiology of osteoarthritis. Osteoarthritis diagnosis and management 1984; 9-27.
3. Whittle J, Steinberg E, Anderson G, Herbert R, Hochberg M. Incidence of and indications for total hip replacement (THR) among elderly Americans. Arthritis Rheum 1990; 33(Suppl.9): S139.
4. Sulzbacher I. Arthrosis-histology and pathogenetic approaches. Radiologe 2000; 40:1126-1133.
5. Radin E, Paul I, Tolkoff M. Subchondral bone changes in patients with early degenerative joint disease. Arthritis Rheum 1970; 13:400-405.
6. Radin E, Rose R. Role of subchondral bone in the initiation and progression of cartilage damage. Clin Orthop 1986; 213:34-40.
7. McKinley TO, Bay BK. Trabecular bone strain changes associated with cartilage defects in the proximal and distal tibia. J Orthop Res 2001; 19:906-913.
8. Dieppe P, Cushnaghan J, Young P, Kirwan J. Prediction of the progression of joint space narrowing in osteoarthritis of the knee by bone scintigraphy. Ann Rheum Dis 1993; 52:557-563.
9. Bullough P, Goodfellow J, O'Connor J. The relationship between degenerative changes and load-bearing in the human hip. J Bone Joint Surg Br 1973; 55:746-758.
10. Goodfellow J, Bullough P. Studies on age changes in human hip joint. J Bone Joint Surg 1968; 50B:222.
11. Otani T, Whiteside LA, White SE. The effect of axial and torsional loading on strain distribution in the proximal femur as related to cementless total hip arthroplasty. Clin Orthop 1993; 292:376-383.
12. Wolff J. Das Gesetz der Transformation der Knochen. 1892.
13. Ruegsegger P, Koller B, Müller R. A microtomographic system for the nondestructive evaluation of bone architecture. Calcif Tissue Int 1996; 58:24-29.
14. Hildebrand T, Ruegsegger P. A new method for the model-independent assessment of thickness in three-dimensional images. J Microsc 1997; 185:67-75.
15. Hildebrand T, Ruegsegger P. Quantification of bone microarchitecture with the structure model index. Comput Methods Biomech Biomed Engin 1997; 1:15-23.
16. Lorensen WE, Cline HE. Marching cubes: a high resolution 3D surface construction algorithm. Comput Graph 1987; 21:163-169.
17. Odgaard A. Three-dimensional methods for quantification of cancellous bone architecture. Bone 1997; 20:315-328.
18. Imhof H, Breitenseher M, Kainberger F, Trattnig S. Degenerative bone disease: cartilage or vascular disease? Skeletal Radiol 1997; 26:398-403.
19. Greenwald AS, O'Connor JJ. The transmission of load through the human hip joint. J Biomech 1971; 4:507-528.
20. Day JS, Ding M, van der Linden JC, Hvid I, Sumner DR, Weinans H. A decreased subchondral trabecular bone tissue elastic modulus is associated with pre-arthritic cartilage damage. J Orthop Res 2001; 19:914-918.
21. Norrdin RW, Kawcak CE, Capwell BA, McIlwraith CW. Subchondral bone failure in an equine model of overload arthrosis. Bone 1998; 22:133-139.